THE PERMEABILITY BARRIER IN MAMMALIAN EPIDERMIS

PETER M. ELIAS and DANIEL S. FRIEND

From the Department of Pathology, University of California, San Francisco, California 94143

ABSTRACT

The structural basis of the permeability barrier in mammalian epidermis was examined by tracer and freeze-fracture techniques. Water-soluble tracers (horseradish peroxidase, lanthanum, ferritin) were injected into neonatal mice or into isolated upper epidermal sheets obtained with staphylococcal exfoliatin. Tracers percolated through the intercellular spaces to the upper stratum granulosum, where further egress was impeded by extruded contents of lamellar bodies. The lamellar contents initially remain segregated in pockets, then fuse to form broad sheets which fill intercellular regions of the stratum corneum, obscuring the outer leaflet of the plasma membrane. These striated intercellular regions are interrupted by periodic bulbous dilatations. When adequately preserved, the interstices of the stratum corneum are wider, by a factor of 5–10 times that previously appreciated. Freeze-fracture replicas of granular cell membranes revealed desmosomes, sparse plasma membrane particles, and accumulating intercellular lamellae, but no tight junctions. Fractured stratum corneum displayed large, smooth, multilaminated fracture faces. By freeze-substitution, proof was obtained that the fracture plane had diverted from the usual intramembranous route in the stratum granulosum to the intercellular space in the stratum corneum. We conclude that: (*a*) the primary barrier to water loss is formed in the stratum granulosum and is subserved by intercellular deposition of lamellar bodies, rather than occluding zonules; (*b*) a novel, intercellular freeze-fracture plane occurs within the stratum corneum; (*c*) intercellular regions of the stratum corneum comprise an expanded, structurally complex, presumably lipid-rich region which may play an important role in percutaneous transport.

The ultimate stage of differentiation in mammalian keratinizing epithelia is the formation of a thin, protective sheath—the stratum corneum. Formerly considered to be merely a mass of sloughing cells, this outermost layer of the epidermis is now recognized to constitute a highly impermeable barrier against water loss and the penetration of substances from the environment (4, 20, 31, 35). Despite its general imperviousness, however, certain substances readily traverse the stratum corneum, hence the concept of selective permeability (4, 31).

Although the stratum corneum possesses a complex array of membrane and extracellular structures not present in subjacent layers (14, 23, 26), current dogma holds that both barrier function and selective transport are subserved by the intracellular fibrillar-matrix complex of the anucleate cornified cell itself (20, 29, 31, 35). That membrane or intercellular components of cornified cells may be functionally important in permeability has been given slight credence. Nevertheless, recent studies have intimated that junctional (16, 34) or intercellular specializations (24, 32, 34) may participate in

the impedient barrier function of keratinizing epithelia.

We performed tracer, thin-section, and freeze-fracture experiments on isolated, intact epidermal sheets in order to: (*a*) identify membrane modifications which occur during keratinization; and (*b*) delineate barrier sites within keratinizing epithelia.

MATERIALS AND METHODS

Animals and Experimental Material

Neonatal mouse skin was used in these experiments because of its homogeneity (it is hairless and ductless), and because after injection of certain phage group II staphylococci (25) it is highly susceptible to midepidermal cleavage with cell-free fractions isolated from these bacteria. In order to obtain intact sheets, 1-3-day old Swiss albino mice were given subcutaneous injections of partially purified exfoliative fractions (1). 2 h later, morphologically intact sheets were peeled from mice previously sacrificed by cervical dislocation, and either processed directly for electron microscopy or perfused with tracers (see below) in a Millipore (Millipore Corp., Bedford, Mass.) chamber before processing for electron microscopy.

Tracer Studies In Vivo and In Vitro

Horseradish peroxidase (HRP) (50 mg/ml N saline) (Sigma Chemical Co., St. Louis, Mo., or Worthington Biochemical Corp., Freehold, N.J.), thorium dioxide, 3% lanthanum nitrate in 0.05 M Tris HCl buffer, or N saline alone were topically applied or intradermally injected into neonatal mice about 20–30 min before biopsy. For in vitro studies, isolated epidermal sheets were spread (either stratum corneum or stratum granulosum layer up) over a Millipore filter and perfused for several minutes with HRP (5–25 mg/ml N saline) or horse spleen ferritin (Pentex Biochemical, Kankakee, Ill.). All in vivo or in vitro perfused specimens were processed as described below for electron microscopy.

Electron Microscopy

After fixation in cacodylate-buffered glutaraldehyde for 5 h at room temperature, specimens were postfixed for 1.5 h in 1% Veronal-buffered OsO_4 at 0–4°C, washed in 1.5% uranyl acetate in Michaelis buffer (pH 6.0), dehydrated, and embedded in Epon. Some specimens were fixed with osmium vapor alone and then processed as above. After glutaraldehyde fixation, HRP-perfused specimens were sectioned with a tissue chopper, incubated with diaminobenzidine according to the method of Graham and Karnovsky (15), and postfixed in OsO_4 containing potassium ferrocyanide (19). Thin sections were stained with uranyl acetate and lead citrate and examined in either a Zeiss EM9S or Siemens 1A electron microscope.

Freeze-Fracture, Freeze-Etching, and Freeze-Substitution

Full-thickness skin and sheets were fixed for 1–2 h in cacodylate-buffered glutaraldehyde, then cryoprotected with 20% glycerol in buffer for 2–16 h, mounted on cardboard disks, and fractured at −115°C in a Balzer's freeze-etch apparatus (Balzer's High Vacuum Corp., Santa Fe, Calif.). Some specimens were fixed for 1 h in OsO_4 rather than in glutaraldehyde and then processed as described above. Other specimens were treated with 5% or 10% glycerol, fractured, and subsequently etched at −100°C for 1–5 min before shadowing. Replicas were cleaned by sequential treatment with absolute methanol and triple-strength Chlorox.

In order to localize the cleavage plane in the stratum corneum more precisely, we fractured several samples and then freeze-substituted them (−70°C) in 2% OsO_4 in absolute acetone (17). After 3 days, the specimens were slowly brought to room temperature over the course of several hours, then dehydrated, embedded, and sectioned perpendicular to the cleavage plane.

Stereology

The volumetric contribution of lamellar bodies to the stratum granulosum was assessed stereologically by utilizing a regular grid superimposed on randomly selected micrographs enlarged to constant (× 50,000) magnification. The formula $P_P = V_V$ permits extrapolation of point intersections to relative volume, provided that sections are considerably thinner than object(s) being studied, and that a large, random selection of sections is utilized (12). Tissue postfixed in potassium ferrocyanide was used because after such treatment lamellar granules could be much more readily discerned than in routinely prepared material.

RESULTS

An Overview of Epidermal Morphological Differentiation

The following paragraph summarizes the essential cytological features of keratinization. For more extensive reviews of the cellular events accompanying epidermal differentiation, see references 5 and 7.

Keratinocyte differentiation begins in the germinative or basal layer, where most of the epidermal intracellular filamentous protein is synthesized. As postmitotic daughter cells migrate apically through the stratum spinosum, they become more cuboidal in contour; protein synthesis continues, and filaments aggregate into bundles of fibrils. In the stratum granulosum, preceding transformation into cornified cells, the cells flatten, begin to

synthesize keratohyalin, recycle most of their nucleic acids, and extrude myriad small lamellar granules (Odland bodies, membrane-coating granules) into the intercellular space. The anucleate cells of the stratum corneum lack recognizable organelles and inclusions other than keratin filaments in an amorphous matrix. The cell membrane of the cornified cell thickens strikingly with the deposition of a dense zone beneath the plasma membrane, while the intercellular space appears to vary greatly in both width and content.

Structural Features of Barrier Strata

THE STRATUM GRANULOSUM: In neonatal mouse epidermis, the stratum granulosum is four to six cell layers thick. Here the cells contain multiple ellipsoid granules, measuring 0.2–0.3 μm, which contain parallel 40-Å lamellae in an amorphous matrix (Fig. 1 *a*, *b*). Stereological measurements indicate that lamellar bodies may occupy as much as 15% (range: 2%–15%) of the granular cell cytoplasm. Individual lamellar granules take form in Golgi regions of he upper stratum spinosum and lower stratum granulosum, subsequently aggregate in the peripheral cytoplasm, then eject their contents into the intercellular space, and progressively accumulate within focal interdesmosomal dilatations and deep invaginations of the cell membrane (Fig. 1 *a*, *b*). After expulsion into the intercellular space, lamellae initially remain segregated in packets, then fuse to form broad sheets (Fig. 1 *a*, *b*).

Freeze-fracture images confirm that intra- and intercellular lamellar granules have a similar laminated substructure. These replicas also provide additional visual evidence of the ubiquity and ellipsoid shape of these bodies (Fig. 2). Like mitochondria, lamellar bodies tend to fracture through the outer limiting membrane, and such replicas reveal no substructure. The degree of engorgement of the intercellular space by discharged lamellae can also be best appreciated in fractured specimens (Figs. 2 and 4). Within the intercellular space, adjacent lamellae tend to fuse into broad sheets (Figs. 1 *b*, 2, 4, and 5).

In thin section, plasma membranes of the stratum granulosum retain their typical trilaminar structure, punctuated by desmosomes but without evidence of any tight or gap junctions (Fig. 1). Freeze-fractures of the stratum granulosum disclose intramembranous fracture planes with sparse, randomly arranged particles, as well as aggregates of 8–10-nm particles or pits with the dimensions and distribution of desmosomes (Figs. 3, 4).

THE STRATUM CORNEUM: During transition to the stratum corneum, drastic alterations are evident in thin sections of cell membranes. An electron-dense, homogeneous band obscures the inner leaflet of the plasma membrane (Figs. 6, 7) except in the areas beneath desmosomes in the lowest layers of the stratum corneum, where cornified cells often form button-like protrusions. As desmosomes disappear at higher levels, this dense zone is transformed into an uninterrupted sheet approximately 16–20 nm thick. The outer

Abbreviations used in figure legends:
D, Desmosome
DZ, Dense zone
CC, Cornified cell
LB, Lamellar body
IL, Intercellular lamellae
IML, Intramembranous lacuna
KH, Keratohyalin granule
SC, Stratum corneum
SG, Stratum granulosum

FIGURE 1 *a*, *b* Boundary of stratum granulosum and stratum corneum. Granular cells contain numerous intracellular lamellar bodies (*inset*), keratohyalin granules, condensed bundles of tonofilaments, and desmosomes. At this interface, the intercellular space between desmosomes is dilated by extruded lamellar material derived from the exocytosis of lamellar bodies. Much of the lamellar material remains segregated in packets in the intercellular space, while elsewhere lamellar material has fused into broad sheets. Fig. 1 *a*, × 76,000. Fig. 1 *b*, × 119,500.

FIGURE 2 Freeze-fracture replica of upper stratum granulosum and lower stratum corneum. The direction of shadowing is *up* in this figure and in all subsequent replicas. Lamellar bodies migrate apically and laterally in the granular cell, extruding their lamellar contents (arrows) into the intercellular space. Large, particle-free, multilaminated fracture faces predominate in the stratum corneum succeeding typical A and B membrane faces in the stratum granulosum (cf. Figs. 3, 4). Individual lamellar steps correspond approximately to the thickness of disks (4 nm) in the intracellular lamellar bodies (cf. Fig. 1 *a*, *b*). × 60,000.

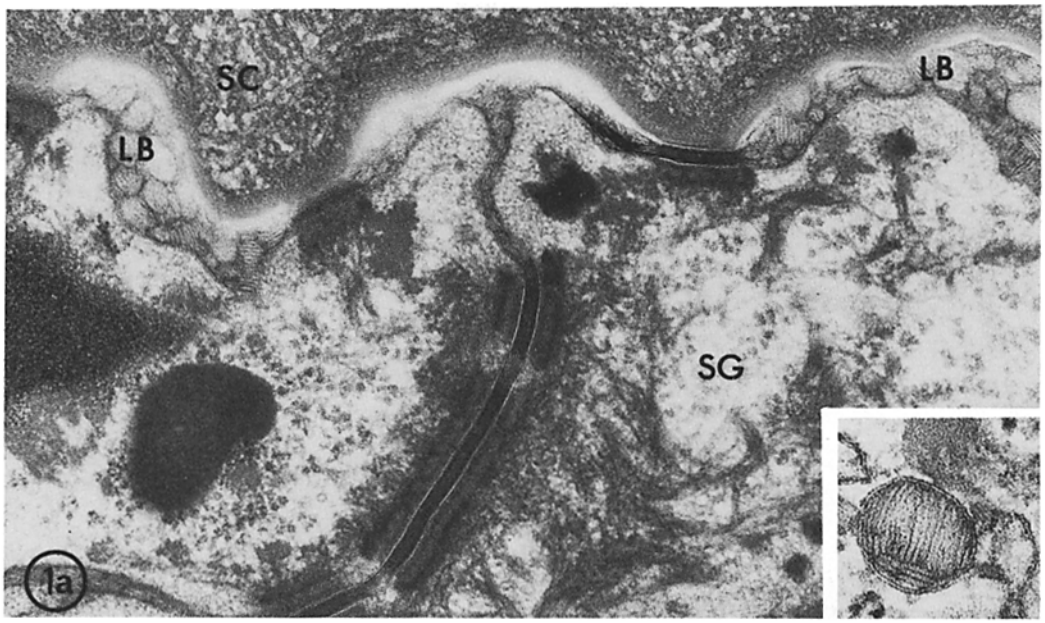
SC
LB
LB
SG
1a


1b

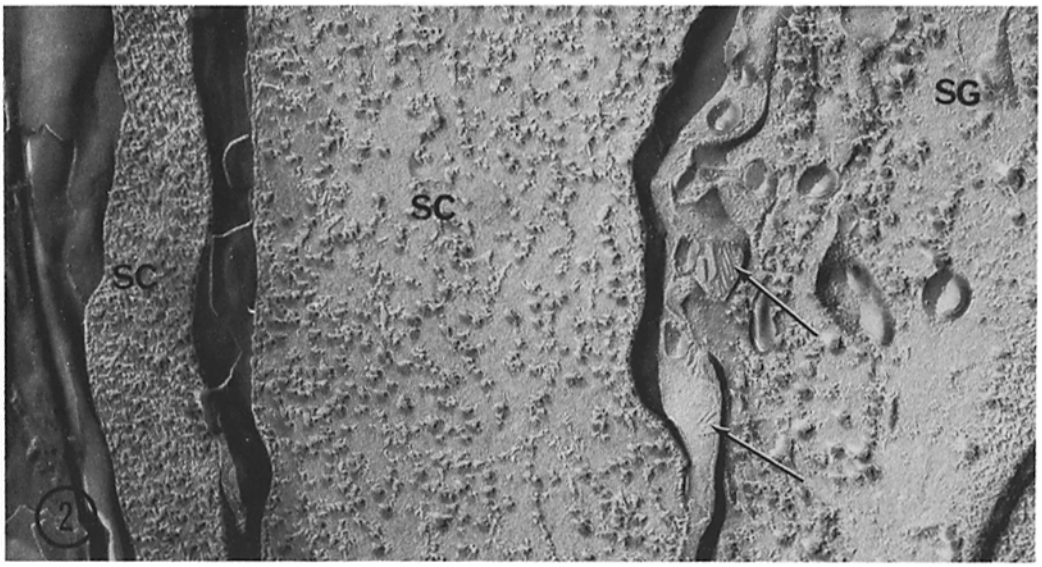
SG
SC
SC
2


D
D
D
3


D
D
4

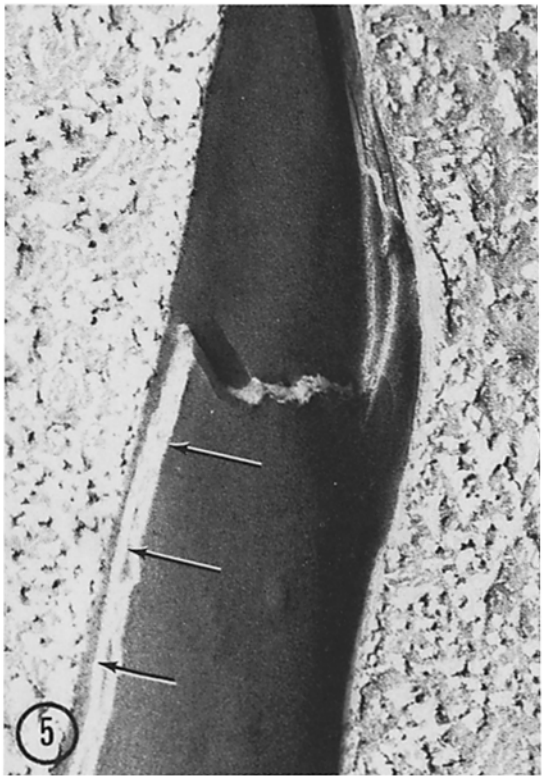
5

leaflet, too, is inconspicuous but evident on close scrutiny in routine preparations where intercellular contents are preserved. Often the outer leaflet appears to fuse with amorphous intercellular material, forming a membrane which frequently becomes detached (Fig. 7). An approximately 5-nm wide electron-lucent zone is consistently present between inner and outer leaflets.

After immersion in *n*-butanol and fixation with osmium vapor alone, portions of the intercellular content of the stratum corneum are preserved. Thin sections reveal a distinctive banded pattern consisting of three to five continuous sheets with intervening bulbous dilatations containing homogeneous, electron-dense material (Figs. 8, 9). The width of the intercellular space spanning adjacent cells under these conditions varies from 60 to 100 nm.

Replicas of stratum corneum display large, smooth, particle-free laminated fracture faces (Figs. 2 and 5). A maximum of four lamellar steps occurred in these regions (Fig. 5), which corresponds with the thin-section images of three or four striations (cf. Figs. 8 and 9). Large membrane fracture faces occur much more frequently than in the subjacent stratum granulosum (Fig. 2).

Localization of the Fracture Plane in the Stratum Corneum

The absence of membrane-associated particles as well as the similarity of lamellar fracture faces in the stratum granulosum to the broad, multilaminated sheets observed both in thin sections and in replicas of the stratum corneum suggest that the fracture plane in the latter case may have shifted from its usual intramembranous pathway to the intercellular space.

To localize the fracture plane in the stratum corneum, we attempted (*a*) to deep-etch, starting from the presumed intercellular space, through to the true plasma membrane. This approach, however, proved infeasible because the lamellar material would not sublimate, regardless of cryoprotection or etching time; (*b*) to examine replicas of osmium-prefixed tissues. Although osmium prefixation produces multiple membrane cross-fractures in other tissues (18), in the stratum corneum we noted no change in the ratio of smooth vs. cross-fractured images. However, membrane constituents adjacent to large, smooth faces were more detectable after prefixation with osmium than with initial glutaraldehyde fixation; and (*c*) to scrutinize freeze-substituted specimens sectioned perpendicular to the fracture plane. Such specimens revealed cross-fractures of cornified cells alternating with definite intercellular cleavage planes (Fig. 10).

Perfusion Studies

INJECTIONS IN VIVO: When tracers were applied topically to neonatal mouse skin, no tracer was discernible beneath the uppermost layers of the stratum corneum in thin sections. After subcutaneous injection, HRP, lanthanum, and thorium dioxide percolated freely upward from the dermis, through the epidermal intercellular space, and on to the *mid-to-upper stratum granulosum* (Figs. 11 *a*, *b*, 12). Egress apical to the upper granular layer was impeded at sites where the contents of lamellar bodies engorged the intercellular space. No tight or gap junctions were apparent here—a finding consistent with the absence of such junctional structures in freeze-fracture material.

IN VITRO EXPERIMENTS: When intact unextracted epidermal sheets were perfused with tracers from above or beneath in a Millipore chamber, tracer was always excluded from individual cells and generally excluded from the sheets except where cornified cells had detached. No tracer entered intercellular spaces between adherent cells (Fig. 13).

FIGURE 3 The membrane A face of a freeze-fractured granular cell reveals sparse, randomly distributed particles and aggregates of 8–10-nm particles corresponding in dimension and distribution to desmosomes. × 25,500.

FIGURE 4 Looking downward at the granular/cornified cell interface, the granular cell A face discloses very few membrane particles and persistent desmosomal aggregates. Smooth lamellar faces abut on partially etched intercellular lamellae. × 58,000.

FIGURE 5 Broad, smooth, multilaminated fracture planes occur throughout the stratum corneum. The cleavage pathway often skips from two to four levels (arrows) within a single fracture face. × 37,500.

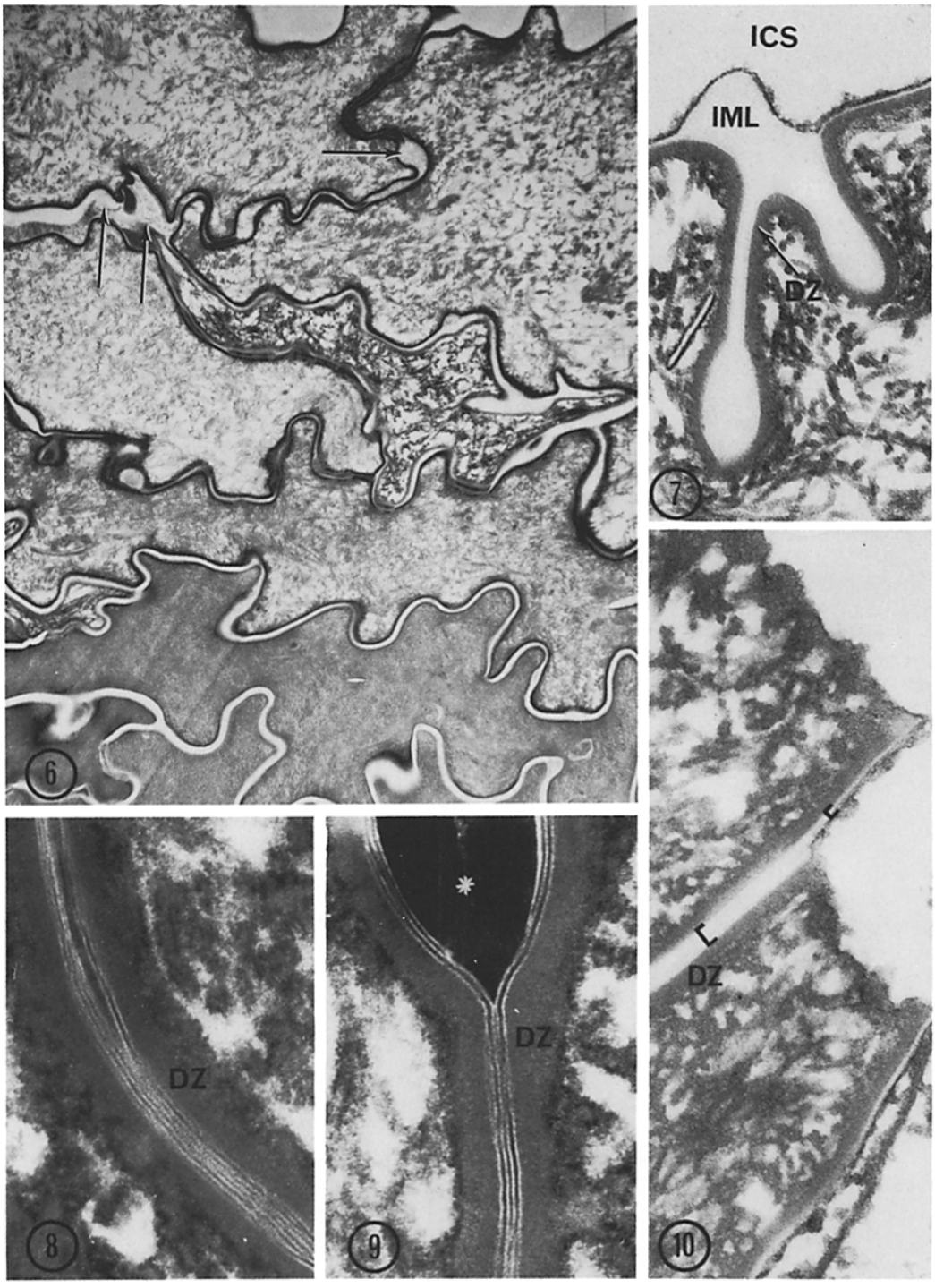
ICS
IML
DZ
6
7
DZ
DZ
DZ
8
9
10

DISCUSSION

The Barrier Function of the Stratum Corneum

Mammals owe their ability to survive in a nonaqueous environment to a barrier against water loss located in the epidermis. A large body of data from in vitro studies indicates that the stratum corneum is a highly impermeable membrane (reviewed in reference 31), and although the observations reported here do not dispute the concept that the stratum corneum is an effective barrier, the results of this study demonstrate that the barrier is actually formed *beneath* the stratum corneum—i.e. in the mid-to-upper stratum granulosum, which may be the primary impediment to body water loss. The structural basis for retardation of water loss appears to be the progressive accumulation of lamellar material, alone or in addition to other substances in the intercellular spaces. Material derived from extruded lamellar granules coalesces to form broad, laminated sheets in the epidermal stratum corneum. The subsequent upward progression of lamellar material throughout the interstices of the stratum probably explains the persistence of impermeability in the stratum corneum, as well as the normal resistance to percutaneous absorption. Exclusion of tracers by intercellular lamellae has been previously noted in other keratinizing epithelia (24, 32, 34), intimating that the functional scheme we describe in this study may indeed apply to most, but not all, mammalian keratinizing epithelia. In amphibian epidermis (13, 21), the corneal epithelium (2) and the wool follicle (28) junctional structures are prominent, possibly because they are so-called transporting epithelia (2). The previous idea that tight junctions are present at the interface of the stratum granulosum and the stratum corneum in mammalian epidermis (16, 34) was not borne out in this investigation: no tight junctions were observed in thin-sectioned or freeze-fractured sheets of neonatal mouse epidermis.

Pathways of Percutaneous Absorption

Although the apical portions of keratinizing epithelia are remarkably impermeable, some substances cross the stratum corneum with relative ease. With the support of mathematical formulae, biophysicists allege that substances traverse cells and intercellular spaces in a nonpreferential manner—i.e. by transcellular pathways (31). This assumption is founded on the premise that the intercellular space is a compartment too narrow, too tortuous, and too inconsequential in volume to explain the observed fluxes across the stratum corneum. Prior ultrastructural studies of the stratum corneum have revealed either narrow intercellular spaces, comparable in dimension to those in other epithelia, or loosely attached cornified cells

FIGURE 6 Thin section of stratum corneum after routine processing for electron microscopy. Anucleate squames have highly irregular, thick cellular envelopes. The intercellular spaces vary in width and content. In the lower stratum corneum (below), the fibrillar cell matrix is compact, whereas distally (above) the matrix appears to have been extracted during tissue processing. In some areas, the intercellular space contains flocculent material (arrows). × 36,000.

FIGURE 7 Cornified cell membranes after routine processing. The inner leaflet of the plasma membrane is obscured by an underlying homogeneous dense zone, 16–20 nm thick. Focal detachment of the outer leaflet produces an intramembranous lacuna. The outer leaflet is also obscured (by adherent, flocculent intercellular material). A central electron-lucent zone (arrows), always present between inner and outer leaflets, is somewhat wider than the central lamina of subjacent granular cell plasma membranes (cf. Fig. 1). × 72,500.

FIGURES 8 and 9 After *n*-butanol treatment and osmium vapor fixation, the intercellular content of the stratum corneum is often preserved (Fig. 8). Three to six 4-nm lamellar striations fill the intercellular space and envelop focal deposits of homogeneous (nonlamellar) electron-dense material (Fig. 9). The inner and outer leaflets of the trilaminar plasma membranes are obscured by the dense zone and intercellular lamellar material, respectively. Fig. 8, × 110,000. Fig. 9, × 111,000.

FIGURE 10 Thin section of cornified cells after freeze-fracture and freeze-substitution. The fractured surfaces are highly osmiophilic. The plane of fracture transects the cornified cells and deviates for short distances through the intercellular space, passing halfway between adjacent cells (brackets). × 18,000.

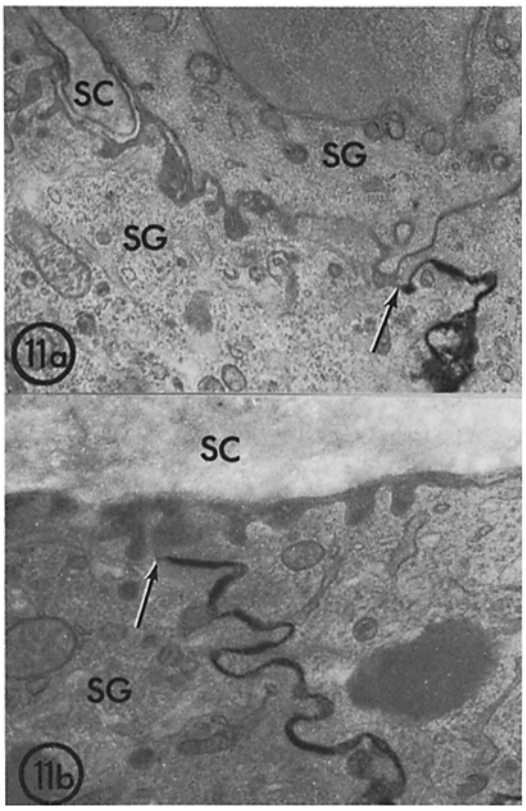
SC
SG
SG
11a
SC
SG
11b

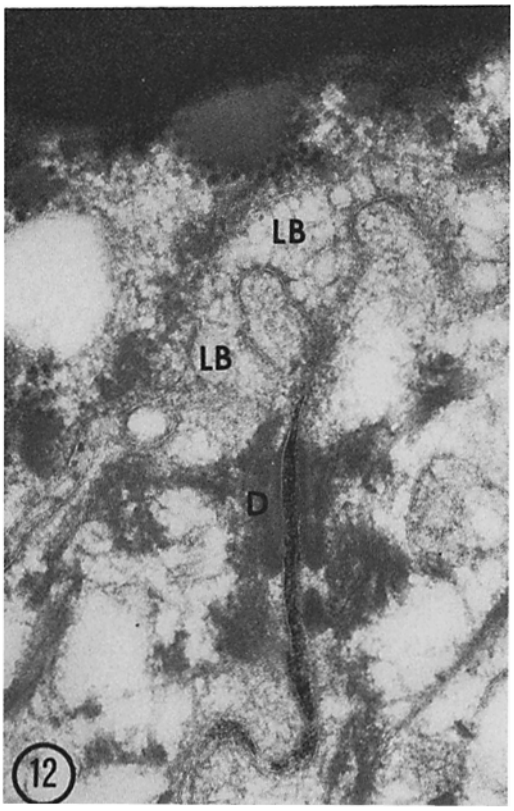
LB
LB
D
12

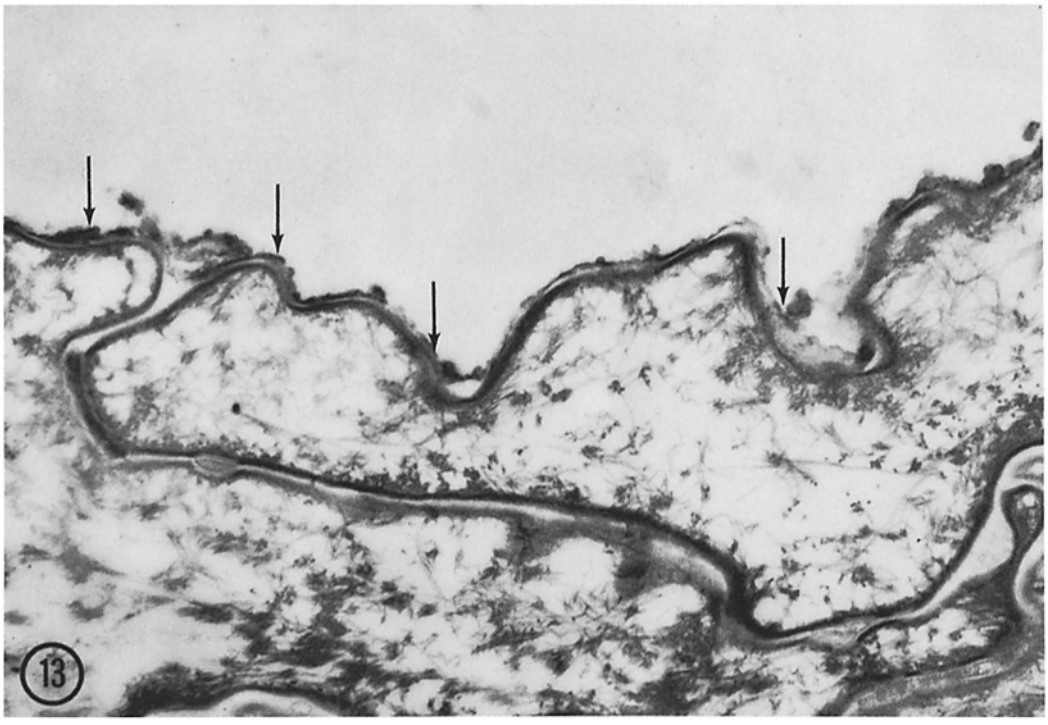
13

separated by wide, often empty spaces (9, 23, 26). As this study has demonstrated, both of these images are artefactual, and are presumably due to extraction occurring during routine processing for electron miscrscopy (8). The more "normal" situation is reflected both by the freeze-fracture images with their stacks of intercellular lamellae, and by the intercellular striations observed in tissues treated with *n*-butanol-osmium vapor (Figs. 8, 9), which are ~80–100 nm wide, compared to the approximately 20-nm space between the plasma membranes of subjacent keratinocytes. The actual volume of the intercellular space may therefore be greater (by a factor of three to seven times) than has yet been appreciated, and may even be greater if the regular, intercellular dilatations are included.

Second, isolated epidermal sheets perfused in vitro with electron-dense tracers confirmed the impermeable nature of intact stratum corneum. Under no circumstances did the water-soluble tracers studied gain access either to individual cornified cells or to the intercellular spaces between adhering cells, except where cells became detached. After treatment with lipid solvents and surfactants, the same tracers penetrate more deeply, once again utilizing intercellular pathways (11, 10). These agents cause increased cell separation, presumably through extraction of intercellular lipid-rich material.

Third, the regularly spaced, bulbous dilatations between adherent cornified cells could have an important function in percutaneous absorption. The lamellar intercellular bands are interrupted by such dilatations (Fig. 9), which are filled with homogeneous, electron-dense material. At the least, these spaces increase the potential volume of the intercellular space. Moreover, they may form a reservoir or network facilitating percutaneous passage of certain substances.

Membrane Structure and Function in Barrier Laminae

The freeze-fracture and thin-sectional picture emerging from these studies establishes that the plasma membrane becomes obscured during its upward progression from the stratum granulosum through the stratum corneum. The inner leaflet of the plasma membrane is obscured by the deposition of a prominent dense zone (3, 13) beneath this leaflet (8, 23, 26). Interestingly, this zone uniformly lines all cornified cells in the stratum corneum with the exception of some cells in the lowest layer, where it is focally absent under desmosomes. Since such desmosomal regions manifest button-like protrusions, it is likely that the principal function of the dense zone is to impart rigidity to individual cornified cells. Recent evidence indicates that the dense zone in mammalian epidermis comprises a fibrillar and amorphous complex significantly different in chemical composition from keratin (22). In thin section, tonofilaments appear to arise in this zone, so that together, the dense zone and intracellular filaments form a continuous ecto- and endoskeleton within the cornified cell. And finally, the outer leaflet may be obscured by intercellular laminae forming a bond with intercellular material. If a bond is formed between intercellular lamellae and outer leaflets, this unit might enhance the stability of the intercellular lamellar network.

Our freeze-fracture observations are similar to those of Breathnach et al. (6) who described similar membrane features in the upper stratum granulosum, but whose description of particle-free plasma membranes in the stratum corneum was, in our opinion, based on images of intercellular lamellae, not upon true membranes. By freeze-substitution, we have shown that the usual cleavage plane in the stratum corneum is intercellular. It

---

FIGURE 11 *a*, *b*. Neonatal mouse epidermis perfused with HRP in vivo. HRP percolates vertically to the upper stratum granulosum, where further egress is blocked (arrows) by the extruded contents of lamellar bodies. Junctional structures are not evident at these levels (cf. Figs. 2–4). (*a*) × 25,000. (*b*) × 27,000.

FIGURE 12 Neonatal mouse epidermis perfused with lanthanum in vivo. Fixation is poor under these conditions, but tracer egress is halted at sites where intercellular spaces become engorged with lamellar bodies. × 64,000.

FIGURE 13 Intact upper epidermal sheet perfused with HRP in vitro. Tracer ingress (arrows) below outer surface is blocked by contiguous cornified cells, a finding identical to that observed after topical application of tracers to neonatal mouse epidermis in vivo. × 42,000.

was our experience that membrane features in the stratum corneum could be visualized on freeze-fracture only after solvent treatment (10, 11). A more complete description of the changes in solvent-treated stratum corneum is in preparation.

Properties of Lamellar Bodies in Keratinizing Epithelia

In neonatal mouse epidermis, multiple lamellar bodies are synthesized and secreted. Because of their extractability with lipid solvents (27) and staining properties (7), and also because of the visual aspect of freeze-fractured lamellae, they are presumably lipid-rich. As lipid packages they presumably deliver hydrophobic materials important for barrier function to the intercellular spaces. Interestingly, they closely resemble the myelin- (5) and phospholipid-rich, surfactant-containing granules of mammalian alveolar Type II cells in freeze-fracture (33). However, numerous other properties have been ascribed to them as well. For example, intracellular lamellar bodies contain several hydrolytic enzymes (36), leading some investigators to consider the extrusion of these bodies to be necessary for the eventual separation and sloughing of superficial cornified cells (37). Quite possibly, lamellar bodies are heterogeneous in function.

Dr. Klaus Wolff of the Division of Experimental Dermatology, I. Hautklinik, University of Vienna, provided invaluable assistance and support during the early phases of this study. We also appreciate the expert technical and editorial aid of Irene Rudolf and Rosamond Michael, respectively.

Portions of this work were presented at the Fourteenth Annual Meeting of the American Society for Cell Biology, San Diego, Calif., 1974.

These studies were supported by United States Public Health Service grant HD-06895 to Dr. Friend, and a Dermatology Foundation fellowship to Dr. Elias.

Received for publication 5 August 1974, and in revised form 9 January 1975.

REFERENCES

1. ARBUTHNOTT, J. P., J. KENT, A. LYELL, and C. G. GEMMELL. 1972. Studies of staphylococcal toxins in relation to toxic epidermal necrolysis (the scalded skin syndrome). *Br. J. Dermatol.* **86** (Suppl. 8):35–39.
2. BERRIDGE, M. J., and J. L. OSCHMAN. 1972. Transporting Epithelia. Academic Press, Inc., New York.
3. BIRBECK, M. S. C., and E. H. MERCER. 1957. The electron microscopy of the human hair follicle. *J. Biophys. Biochem. Cytol.* **3**:215–222.
4. BLANK, I. H. 1969. Transport across the stratum corneum. *Toxicol. Appl. Pharmacol.* Suppl. 3. 23–29.
5. BRANTON, D. 1967. Fracture faces of frozen myelin. *Exp. Cell Res.* **45**:703–707.
6. BREATHNACH, A. S., T. GOODMAN, C. STOLINSKI, and M. GROSS. 1973. Freeze-fracture replication of cells of stratum corneum of human epidermis. *J. Anat.* **114**:65–81.
7. BREATHNACH, A. S., and L. WYLIE. 1966. Osmium iodide positive granules in spinous and granular layers of guinea pig epidermis. *J. Invest. Dermatol.* **47**:58–60.
8. BRODY, I. 1964. Observations on the fine structure of the horny layer in the normal human epidermis. *J. Invest. Dermatol.* **42**:27–31.
9. BRODY, I. 1966. Intercellular space in normal human stratum corneum. *Nature (Lond.)* **209**:472–476.
10. ELIAS, P. M., 1975. Permeability barriers and pathways in mammalian epidermis. *Clin. Res.* **23**:90 A. (Abstr.).
11. ELIAS, P. M., and D. S. FRIEND. 1974. Permeability barriers and pathways in mammalian epidermis. *J. Cell Biol.* **63** (2, Pt. 2):93 a. (Abstr.).
12. ELIAS, H., A. HENNIG, and D. SCHWARTZ. 1971. Stereology: applications to biomedical research. *Physiol. Rev.* **51**:158–200.
13. FARQUHAR, M. G., and G. E. PALADE. 1964. Functional organization of amphibian skin. *Proc. Natl. Acad. Sci. U.S.A.* **51**:569–577.
14. FRITHIOF, L. 1970. Ultrastructural changes in the plasma membrane in human oral epithelia. *J. Ultrastruct. Res.* **32**:1–17.
15. GRAHAM, R. C., JR., and M. J. KARNOVSKY. 1966. The early stages of absorption of injected horseradish peroxidase in the proximal tubules of mouse kidney: ultrastructural cytochemistry by a new technique. *J. Histochem. Cytochem.* **14**:291–302.
16. HASHIMOTO, K. 1971. Intercellular spaces of the human epidermis as demonstrated with lanthanum. *J. Invest. Dermatol.* **57**:17–31.
17. HEREWARD, F. V., and D. H. NORTHCOTE. 1972. Localization of freeze-fracture planes of yeast membranes. *J. Cell Sci.* **10**:555–561.
18. JAMES, R., and D. BRANTON. 1971. The correlation between the saturation of membrane fatty acids and the presence of membrane fracture faces after osmium fixation. *Biochem. Biophys. Acta.* **233**:504–512.
19. KARNOVSKY, M. J. 1971. Use of ferrocyanide-reduced osmium tetroxide in electron microscopy. Proceedings of the 11th Annual Meeting of the American Society for Cell Biology.
20. MALKINSON, F. O. 1964. Permeability of the stratum

corneum. *In* The Epidermis. W. Montagne and W. C. Lobitz, editors. Academic Press, Inc., New York. 435–452.

21. MARTINEZ-PALOMO, A., D. ERLIJ, and H. BRACHO. 1971. Localization of permeability barriers in the frog skin epidermis. *J. Cell Biol.* **50**:277–287.
22. MATOLTSY, A. G. 1974. The substructure and chemical nature of the horny cell membrane. *J. Invest. Dermatol.* **62**:343. (Abstr.).
23. MATOLTSY, A. F., and P. PARAKKAL. 1967. Keratinization. *In* Ultrastructure of Normal and Abnormal Skin. A. S. Zelickson, editor. Lea & Febiger, Philadelphia, Pa. 76–104.
24. MCNUTT, N. S. 1973. Freeze-etch study of plasma differentiation and junctions in a keratinized stratified squamous epithelium. *J. Cell Biol.* **59**:(2, Pt. 2):210 a. (Abstr.).
25. MELISH, M. E., and L. A. GLASGOW. 1970. The staphylococcal scalded skin syndrome—development of an experimental model. *N. Engl. J. Med.* **282**:1114–1119.
26. ODLAND, G. F., and T. H. REED. 1967. Epidermis. *In* Ultrastructure of Normal and Abnormal Skin. A. S. Zelickson, editor. Lea & Febiger, Philadelphia, Pa. 54–75.
27. OLÁH, I., and P. ROHLICH. 1966. Phospholipidgranula in verhornten Ösophagusepithel. *Z. Zellforsch. Mikrosk. Anat.* **73**:205–219.
28. ORWIN, D. F. G., R. W. THOMSON, and N. E. FLOWER. 1973. Plasma membrane differentiations of keratinizing cells of the wool follicles. I–IV. *J. Ultrastruct. Res.* **45**:1–49.
29. ROTHMAN, S. 1954. Physiology and Biochemistry of the Skin. Chicago University Press, Chicago, Ill. 26.
30. RUSHMER, R. F., K. J. K. BEUTTNER, J. M. SHORT, and G. F. ODLAND. 1966. The skin. *Science (Wash. D.C.).* **154**:343–348.
31. SCHEUPLEIN, R. J., and I. H. BLANK. Permeability of the skin. *Physiol. Rev.* **51**:702–747.
32. SCHREINER, E., and K. WOLFF. 1969. Die Permeabilität des epidermalen Intercellularraumes für kleinmolekulares Proteinen. *Arch. Klin. Exp. Dermatol.* **235**:78–88.
33. SMITH, D. S., U. SMITH, and J. W. RYAN. 1972. Freeze-fractured lamellar body membranes of the rat lung great alveolar cell. *Tissue Cell* **4**:457–468.
34. SQUIER, C. A. 1973. The permeability of keratinized and nonkeratinized oral epithelium to horseradish peroxidase. *J. Ultrastruct. Res.* **43**:160–177.
35. TREGEAR, R. 1966. Physical Functions of Skin. Academic Press, Inc, London. 1–52.
36. WEINSTOCK, M., and G. F. WILGRAM. 1970. Fine structural observations on the formation and enzymatic activity of keratinosomes in mouse filiform papillae. *J. Ultrastruct. Res.* **30**:262–274.
37. WOLFF, K., and K. HOLUBAR. 1967. Keratinosomen als epidermale lysosomen. *Arch. Klin. Exp. Dermatol.* **231**:1–19.